Fourier phase microscopy for investigation of biological structures and dynamics

Gabriel Popescu, Lauren P. Deflores, and Joshua C. Vaughan

George R. Harrison Spectroscopy Laboratory, Massachusetts Institute of Technology, Cambridge, Massachusetts 02139

Kamran Badizadegan

Harvard Medical School and Massachusetts General Hospital, Boston, Massachusetts 02114

Hidenao Iwai

Photonics K.K., Hamamatsu, Shizuoka 430-8587, Japan

Ramachandra R. Dasari and Michael S. Feld

George R. Harrison Spectroscopy Laboratory, Massachusetts Institute of Technology, Cambridge, Massachusetts 02139

Received May 26, 2004

By use of the Fourier decomposition of a low-coherence optical image field into two spatial components that can be controllably shifted in phase with respect to each other, a new high-transverse-resolution quantitative-phase microscope has been developed. The technique transforms a typical optical microscope into a quantitative-phase microscope, with high accuracy and a path-length sensitivity of $\lambda/5500$, which is stable over several hours. The results obtained on epithelial and red blood cells demonstrate the potential of this instrument for quantitative investigation of the structure and dynamics associated with biological systems without sample preparation. © 2004 Optical Society of America

OCIS codes: 180.0180, 170.1530.

Phase-contrast and differential interference-contrast microscopy provide high-contrast intensity images of transparent biological structures without sample preparation.[1,2] However, although these techniques reveal the structure of the sample, the phase information provided is qualitative. Phase-shifting interferometry (PSI) is commonly used for quantitative metrology,[3] and interferometric techniques based on this principle have been demonstrated for fast imaging.[4] Digital holography has also been developed for phase-contrast imaging[5] and integrated with PSI.[6]

Recently, by using two harmonically related wavelengths, our group developed an interferometric technique for single-point phase measurements and demonstrated its potential for cell biology studies.[7] A phase-imaging instrument that combines a stereo microscope with PSI was used for biological applications.[8] However, this experimental arrangement does not take any precautions to suppress phase noise, which may affect the long-term stability of the instrument. A noninterferometric technique based on the irradiance transport equation was also developed for extracting optical phase images.[9] This method requires displacement of the sample through the focus and requires extensive computations, which may limit its applicability to dynamic biological studies.

The description of an optical image as an interference phenomenon was noted by Abbe more than 125 years ago[10] and represents the underlying principle of phase-contrast microscopy.[1] In this spirit, Kadono *et al.*[11] developed a phase-shifting interferometer that is based on the interference of the scattered and unscattered light from transparent samples. In that setup the sample was illuminated by a laser and stability was achieved due to the common optical path for interfering beams. In addition to collecting the typical PSI four-frame interferograms, the phase image reconstruction required the measurement of the unscattered field amplitude, which imposed drastic restrictions on the system alignment. Recently, a similar system was combined with oblique illumination to enhance optical resolution.[12]

In this Letter we present a highly sensitive phase-imaging instrument, referred to as the Fourier phase microscope (FPM), which relies on the similar principle of decomposing a given field into its average and a spatially varying field. In our setup the two interfering fields are derived by Fourier transforming the output image of an existing transmission microscope, which provides excellent transverse resolution and long-term stability. The experimental setup is depicted in Fig. 1. The low-coherence field from a superluminescent diode (center wavelength of 809 nm and bandwidth of 20 nm) is used as the illumination source for a typical inverted microscope (Axiovert 35, Carl Zeiss, Inc.). To ensure full spatial coherence, the light was coupled into a single-mode fiber and subsequently collimated, such that essentially plane-wave illumination of the sample was achieved. Through the video port, the microscope produces a magnified image positioned at image plane IP, which appears to be illuminated by virtual point source VPS. Correcting lens CL is positioned at the

0146-9592/04/212503-03$15.00/0

same plane IP and has a focal length such that it images VPS at infinity. Thus the new image formed by CL preserves the magnification and position of the original microscope image, while it appears to be illuminated by a plane wave. The image field formed by CL can now be Fourier transformed as in standard 4-f geometries. The Fourier transform of the image field is projected by Fourier lens FL (50-cm focal distance) onto the surface of programmable phase modulator PPM (X8267 Hamamatsu Photonics K.K., 768 × 768 active pixels). PPM consists of an optically addressed, two-dimensional liquid-crystal array. Polarizer P adjusts the field polarization on a direction parallel to the molecular axis of the liquid crystal. In this configuration PPM produces precise control over the phase of the light reflected by its surface. The PPM pixel size is 26 μm × 26 μm, and the dynamic range of the phase control is 8 bits over 2π. In the absence of programmable phase modulation, an exact phase and amplitude replica of the image field is formed at the CCD plane by means of beam splitter BS. PPM is used to controllably shift the phase of spatially varying field component E_1 (solid curve in Fig. 1) in four increments of $\pi/2$ with respect to average field E_0 (dotted curve), as in typical PSI measurements.[3] The center modulation region on PPM is a circle with a diameter of 8 pixels, which ensures that E_0 is uniform in the image plane. The phase image retrieval rate is limited by the refresh rate of PPM, which in our case is 8 Hz.

In the image plane, E_1 interferes at each point with uniform field E_0, and the irradiance image recorded by the CCD as a function of the phase increment has the form

$$I(x,y;n) = |E_0|^2 + |E_1(x,y)|^2 + 2|E_0|\,|E_1(x,y)| \times \cos[\Delta\phi(x,y) + n\pi/2], \qquad n = 0,1,2,3. \tag{1}$$

In Eq. (1), $\Delta\phi$ represents the phase difference between E_0 and E_1 and is retrieved from the four interferograms by means of $\tan(\Delta\phi) = [I(3) - I(1)]/[I(0) - I(2)]$. The phase distribution associated with the microscope image, the quantity of interest, can be expressed as the phase of the complex sum $E_0 + E_1(x, y)$:

$$\phi(x,y) = \tan^{-1}\left\{\frac{\beta(x,y)\sin[\Delta\phi(x,y)]}{1 + \beta(x,y)\cos[\Delta\phi(x,y)]}\right\}, \tag{2}$$

with $\beta(x, y) = |E_1(x, y)|/|E_0|$. Since E_0 is essentially a plane wave, parameter β can be extracted from the four frames of Eq. (1) up to a multiplicative constant $\gamma = 1/4\,|E_0|^2$:

$$\beta(x,y) = \gamma\,\frac{[I(x,y;0) - I(x,y;2) + I(x,y;3) - I(x,y;1)]}{\sin[\Delta\phi(x,y)] + \cos[\Delta\phi(x,y)]}. \tag{3}$$

Equation (1) also provides two analytical solutions for β: β_1 and $\beta_2 = 1/\beta_1$. However, in the limit $\phi \to 0$ the physically valid solution for β is $\beta_1 \to 0$. Thus the relevant value of γ can be obtained by evaluating the expression on the right-hand side of Eq. (3) at points (x_0, y_0), where it has small values, and imposing $\beta(x_0, y_0) = \beta_1(x_0, y_0)$. The quantity $\phi(x, y)$ is therefore uniquely determined from the four interferograms with no additional measurements or inherent experimental complications. The measurement is not particularly sensitive to the size of the modulated region on PPM, given that E_0 is uniform over the field of view.

To study the accuracy and sensitivity to small phase changes of the FPM, various calibrated samples were investigated. Figure 2 shows an example of such measurements, obtained from imaging polystyrene microspheres. To better simulate a transparent biological sample, the spheres were immersed in 100% glycerol and sandwiched between two coverslips, such that the refractive-index contrast achieved between the particles and the surrounding medium was $\Delta n = 0.12$. The diameter of the particles was 2.97 ± 0.045 μm, as provided by the manufacturer (Duke Scientific).

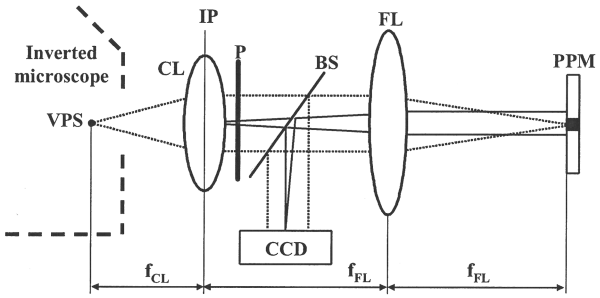

Fig. 1. Experimental setup.

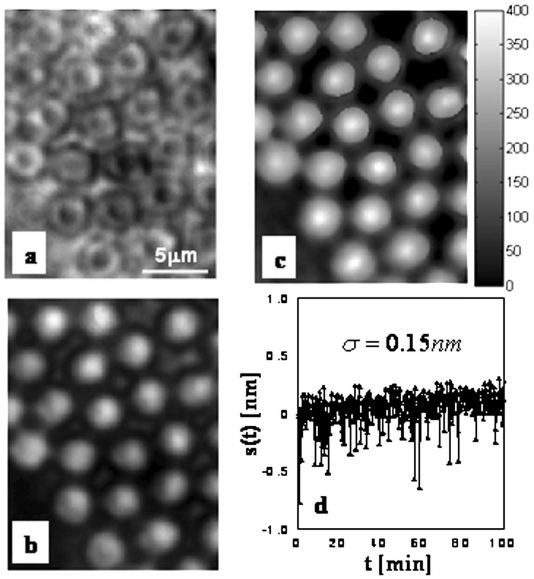

Fig. 2. Experimental results for polystyrene microspheres in glycerol by use of a 10× microscope objective: a, intensity image; b, phase-contrast image; c, FPM image. The gray-scale bar represents the path-length shift in nanometers. d, Optical path-length temporal fluctuations in the absence of particles.

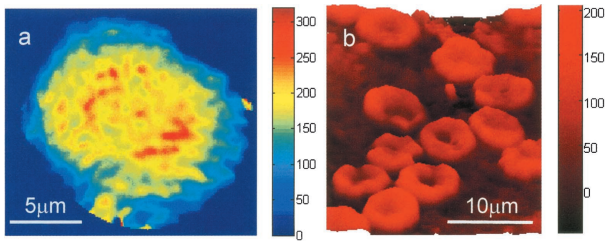

Fig. 3. FPM images obtained with a 40× microscope objective: a, phase image of a HeLa cell undergoing mitosis; b, phase image of whole blood smear. The color bars represent optical path length in nanometers.

Thus the expected optical path-length shift through the microspheres had a value of 365 ± 5 nm. With no modulation on PPM a transmission intensity image was obtained (Fig. 2a). The contrast of this image is poor due to the transparency of the sample. Figure 2b shows the phase-contrast image, obtained by use of a $\pi/2$ phase shift on PPM. Although this image shows improved contrast, it does not provide the thickness of the sample. The FPM image (Fig. 2c) exhibits high contrast and provides quantitative information about the sample thickness. The measured optical path-length shift through the microspheres was 350 ± 26 nm, which agrees well with the values indicated by the manufacturer. The uncertainty in our measurement might be due to impurities present in the solution and residual imperfections of the imaging beam.

To assess the stability of the instrument against phase noise and thus quantify its sensitivity to optical path-length changes, a cell chamber containing only water (no particles) was continuously imaged at intervals of 15 s. Figure 2d shows the temporal optical path-length fluctuations associated with a point contained in the field of view over a 100-min period; the CCD exposure time was 50 ms for each interferogram. The phase was averaged over an area of 0.6 μm × 0.6 μm, which corresponds to the transverse resolution of the microscope. The standard deviation of these fluctuations had a value of $\sigma = 0.15$ nm, which is equivalent to $\lambda/5500$. This result demonstrates the remarkable path-length sensitivity of the FPM and its potential for investigating long-term time-varying processes. The extremely low noise is due to the fact that the two interfering fields traverse a common optical path. In addition, Fourier processing is performed on a magnified microscope image of the sample, which further narrows the optical path of the interfering fields and also provides improved mechanical stability. The use of a low-coherence illumination field, as opposed to laser radiation, contributes to the sensitivity of the method, because fringes created by multiple reflections on various components are suppressed.

The FPM was further applied to image live cells. HeLa cells (an epithelial cell line derived from a cervical neoplasm) were continuously monitored over periods of up to 12 h at repetition rates of 4 frames/min. Figure 3a shows the color-coded quantitative-phase image of a cell during the metaphase of mitosis, revealing the structure of separating chromatids. The cells were imaged in typical culture conditions (i.e., immersed in culture medium), and no preparation was performed before the measurement. This facilitates the quantitative analysis of cellular dynamics such as shape change or growth over long periods of time.

Figure 3b shows the pseudocolor quantitative-phase image of a whole blood smear. The sample was prepared by sandwiching a small drop of fresh blood between two coverslips. The well-known discoid shape of red blood cells is recovered. Simple analysis that takes into account the refractive index of hemoglobin with respect to plasma can easily provide information about the volume of red blood cells. The FPM can therefore provide a high-throughput procedure for screening various abnormalities in red cells and potentially other blood constituents.

In summary, the FPM provides a nonperturbative means of accurately measuring phase images of cells and other biological structures in their natural states without sample preprocessing. Its high stability allows for time-varying processes to be studied over periods of many hours.

This work was carried out at the Massachusetts Institute of Technology Laser Biomedical Research Center, supported by National Institutes of Health grant P41 RR 02594, and partially supported by Hamamatsu Photonics K.K. G. Popescu's e-mail address is gpopescu@mit.edu.

References

1. F. Zernike, Physica **9,** 686 (1942).
2. F. H. Smith, Research (London) **8,** 385 (1955).
3. K. Creath, in *Progress in Optics*, E. Wolf, ed. (North-Holland, Amsterdam, 1988), Vol. 26, p. 349.
4. A. Dubois, L. Vabre, and A. C. Bocara, Opt. Lett. **26,** 1873 (2001).
5. E. Cuche, F. Bevilacqua, and C. Depeursinge, Opt. Lett. **24,** 291 (1999).
6. I. Yamaguchi and T. Zhang, Opt. Lett. **22,** 1268 (1997).
7. C. Yang, A. Wax, M. S. Hahn, K. Badizadegan, R. R. Dasari, and M. S. Feld, Opt. Lett. **26,** 1271 (2001).
8. G. A. Dunn and D. Zicha, in *Cell Biology: a Laboratory Handbook*, 2nd ed., J. Celis ed. (Academic, San Diego, Calif., 1997), pp. 44–53.
9. D. Paganin and K. A. Nugent, Phys. Rev. Lett. **80,** 2586 (1998).
10. E. Abbe, Arch. Mikrosk. Anat. Entwicklungsmech. **9,** 431 (1873).
11. H. Kadono, M. Ogusu, and S. Toyooka, Opt. Commun. **110,** 391 (1994).
12. A. Y. M. Ng, C. W. See, and M. G. Somekh, J. Microsc. **216,** 334 (2004).